Harnessing the Hofmeister Effect for Dynamic Self-Assembly of Supramolecular Hydrogels

Tang, Hongwang; Gao, Yuliang; Zhang, Jiahao; Li, Zhongqi; Gao, Qi; Cai, Peiwen; Chen, Xinyu; Guo, Xuhong; van Esch, Jan H.; Wang, Yiming

DOI
10.1002/anie.202505417

Publication date
2025

Document Version
Final published version

Published in
Angewandte Chemie - International Edition

How to cite: *Angew. Chem. Int. Ed.* **2025**, *64*, e202505417
doi.org/10.1002/anie.202505417

Supramolecular Hydrogels **Hot Paper**

Harnessing the Hofmeister Effect for Dynamic Self-Assembly of Supramolecular Hydrogels

Hongwang Tang, Yuliang Gao, Jiahao Zhang, Zhongqi Li, Qi Gao, Peiwen Cai, Xinyu Chen, Xuhong Guo, Jan H. van Esch, Yiming Wang, and Fu-Zhen Xuan**

Abstract: Dynamic regulation of intermolecular interactions is essential for the creation of dynamic supramolecular materials with lifelike self-regulating functions. Yet specific ion effect, which is known to possess potent effect on intermolecular interactions, has remained unexplored for such a purpose. Here, we demonstrate our access to dynamic self-assembly of supramolecular hydrogels by orchestrating the Hofmeister effect through a simple enzymatic reaction. The involved gelators containing carboxylate moieties self-assemble into hydrogel (Gel1) at acidic pH and dissolve at basic pH. We surprisingly find that the dissolved gelators at basic pH can be driven to self-assemble into hydrogel (Gel2) by kosmotropic ions through the disruption of gelator–water interactions. By coupling to the enzymatic hydrolysis of urea, Gel1 gradually disintegrates over time because of the production of basic NH_3. However, interestingly, with the accumulation of kosmotropic ions, NH_4^+ and CO_3^{2-}, the dissolved gelators are driven to self-assemble into Gel2, realizing a self-regulating gel–sol–gel transition process. The transition rate and stiffness of Gel2 are tunable by adjusting the concentrations of urea or urease. This work may shed light on the creation of lifelike self-regulating supramolecular materials using Hofmeister effect for many enticing applications such as ion-programmed biosensing and drug delivery.

Introduction

Hofmeister effect, first recognized by Franz Hofmeister in 1888, describes the effect of specific ions on the solubility of biomacromolecules in aqueous solution that follows a recurring trend known as the Hofmeister series.[1,2] According to the solubility effect, the ions are categorized into kosmotropes and chaotropes. Typically, kosmotropic ions, such as CO_3^{2-} and SO_4^{2-}, closer to the left of the Hofmeister series lead to lower solubility of the solutes, while chaotropic ions, such as I^- and SCN^-, closer to the right lead to higher solubility.[3–5] This behavior is more significant for anions than cations and is thought to be caused by ion-reorganized hydration in bulk or direction interactions between the ions and solutes.[6–10] Over the past two decades, Hofmeister effect has been exploited as a powerful approach to control supramolecular self-assembly by tuning intermolecular interactions, leading to various impressive self-assembling outcomes such as hydrogels,[11,12] micelles,[13] nanorods,[14,15] and MOFs.[16] However, so far, the vast majority of the resultant supramolecular products are usually static without the ability to dynamically evolve their structures and functions against time.[17]

Inspired by the non-equilibrium self-assembly phenomenon in biology, chemists have coupled molecular self-assembly with nonequilibrium chemical reaction networks,[18–22] giving rise to highly dynamic supramolecular architectures such as fibrils,[23,24] vesicles,[25–28] gels,[29–33] and droplets.[34–36] The main mechanism involves the use of high-energy chemicals, such as methylation reagents,[37,38] carbodiimides,[39–42] ATP,[43–47] and pH regulators,[48–51] to change the intermolecular interactions by altering the chemical structure or binding to the building blocks, thereby activating the self-assembly; with the spontaneous dissipation of chemical energy, the intermolecular interactions will recover to the original state, therefore leading to spontaneous collapse of the formed supramolecular structures. Relying on similar mechanism, other beautiful dynamic self-assembly systems driven by light,[52–55] electricity,[56,57] CO_2,[58–60] and reaction-diffusion[61–65] are also reported. Despite these advances, access to dynamic supramolecular self-assembly using Hofmeister effect, a powerful way to regulate intermolecular interactions, remain rarely explored. The achievement of this goal will not only offer new opportunity toward dynamic supramolecular materials with self-regulating functions but also further our understanding of the dynamic self-assembly in biological realm as many

[*] H. Tang, Y. Gao, J. Zhang, Z. Li, Q. Gao, P. Cai, X. Chen, X. Guo, Y. Wang
State Key Laboratory of Chemical Engineering, East China University of Science and Technology, Meilong Road 130, Xuhui, District, Shanghai 200237, P.R. China
E-mail: yimingwang@ecust.edu.cn

Y. Wang, F.-Z. Xuan
Shanghai Key Laboratory for Intelligent Sensing and Detection Technology, East China University of Science and Technology, Meilong Road 130, Xuhui, District, Shanghai 200237, P.R. China
E-mail: fzxuan@ecust.edu.cn

J. H. van Esch
Department of Chemical Engineering, Delft University of Technology, Van der Maasweg 9, 2629 HZ, Delft, The Netherlands

Additional supporting information can be found online in the Supporting Information section

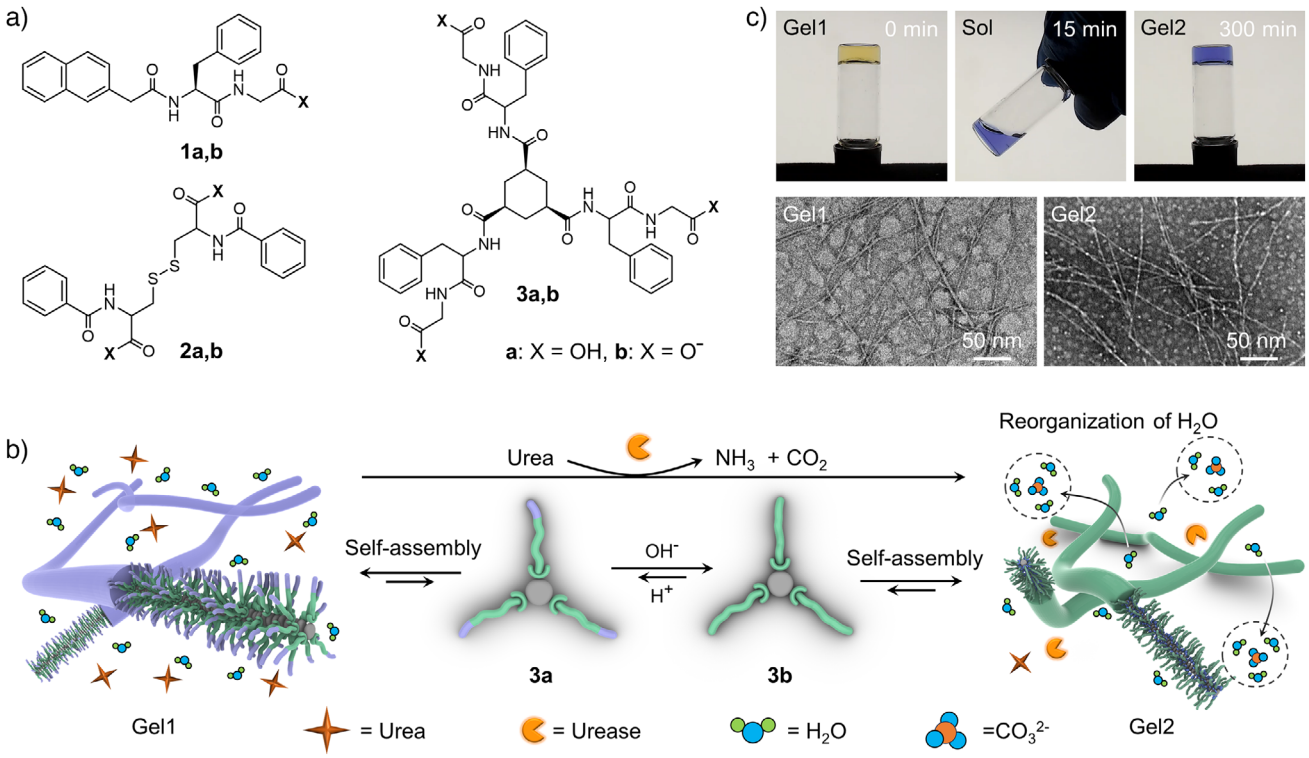

Figure 1. Hofmeister effect–mediated dynamic supramolecular hydrogelation. a) Chemical structures of gelators **1**, **2**, and **3**. b) Illustration of the self-assembly of gelator **3** into Gel1 through protonation, and the transition process from Gel1 to sol, and eventually to Gel2 relying on the enzymatic production of basic NH_3 and kosmotropic ions, NH_4^+ and CO_3^{2-}. c) Typical sample showing the dynamic gel–sol–gel transition process and the TEM images of Gel1 and Gel2 of gelator **3**. Sample in (c): initial pH 5.0, [**3a**] = 60 mM, [urea] = 1.0 M, [urease] = 0.16 mg mL^{-1}, and [bromocresol purple] = 50 μM (pH indicator).

self-assembly processes in living system are associated with ions.[66,67]

Here, we present how the Hofmeister effect can be orchestrated to realize dynamic self-assembly of supramolecular hydrogels *via* a rather simple enzymatic reaction (Figure 1). The involved gelators containing different carboxylate moieties (**1**–**3**) self-assemble into supramolecular hydrogels (Gel1) at pH lower than the pK_a of their carboxylates (~4.5) due to the removal of charges by protonation (**1a**–**3a**), while disassemble at pH > pK_a due to the occurrence of deprotonation (**1b**–**3b**) of the gelators, which increases their electrostatic repulsion and solubility (Figures 1a and S1–S3). To our surprise, with the addition of kosmotropic ions, like CO_3^{2-} and SO_4^{2-}, **1b**, **2b**, and **3b** in the solutions with pH > pK_a can be driven to self-assemble into self-supporting hydrogels (Gel2) (Figure S4) due to the disruption of gelator–water interactions by the kosmotropic anions (Figure 1b). In this study, gelator **3** was selected for in-depth investigation in considering of its high sensitivity to kosmotropic ions even at rather high pH (pH 10) and its transparency for easy following (Figure S5). Interestingly, by coupling the self-assembly of gelator **3** to the enzymatic hydrolysis of urea, Gel1 of **3a**, consisting of fibers with a diameter of ~11 nm, gradually converts to solution of **3b** over time because of the production of basic NH_3; however, with the accumulation of kosmotropic ions, NH_4^+ and CO_3^{2-}, dissolved **3b** is further driven to self-assemble into Gel2 composed of fibers with a diameter of ~10 nm (Figure 1b,c), realizing a self-regulating gel–sol–gel transition.

Results and Discussion

To explore whether the Hofmeister effect can be harnessed to realize dynamic supramolecular self-assembly, we first investigated the effect of different ions on the intermolecular interactions by testing the self-assembly behavior of the gelators. In a typical experiment, 60 mM aqueous solutions of gelator **3b** were prepared, and the pH was kept at 8.0 to avoid formation of any preaggregations (Figure S6). To the solutions, a series of anions (sodium salts) at different concentrations were added. To our surprise, the addition of 1.0 M CO_3^{2-} results in rapid formation of self-supporting hydrogel within a couple of seconds (Movie S1), indicating that kosmotropic anions can indeed drive the self-assembly of **3b** though it stays at a deprotonated state. Fast hydrogelations were also observed in other samples with kosmotropic anions, resulting in robust hydrogels with a storage modulus (G') exceeding 10^5 Pa (Figure S7). More importantly, the critical concentration of the kosmotropic anions for hydrogelation of **3b** increases from ~1.0 to ~3.0 M along the sequence of $CO_3^{2-} < SO_4^{2-} < H_2PO_4^- < HPO_4^{2-} < Ac^- < Cl^- < Br^-$, which nicely matches the Hofmeister series (Figure 2a). In contrast, no hydrogelation was observed in the samples with

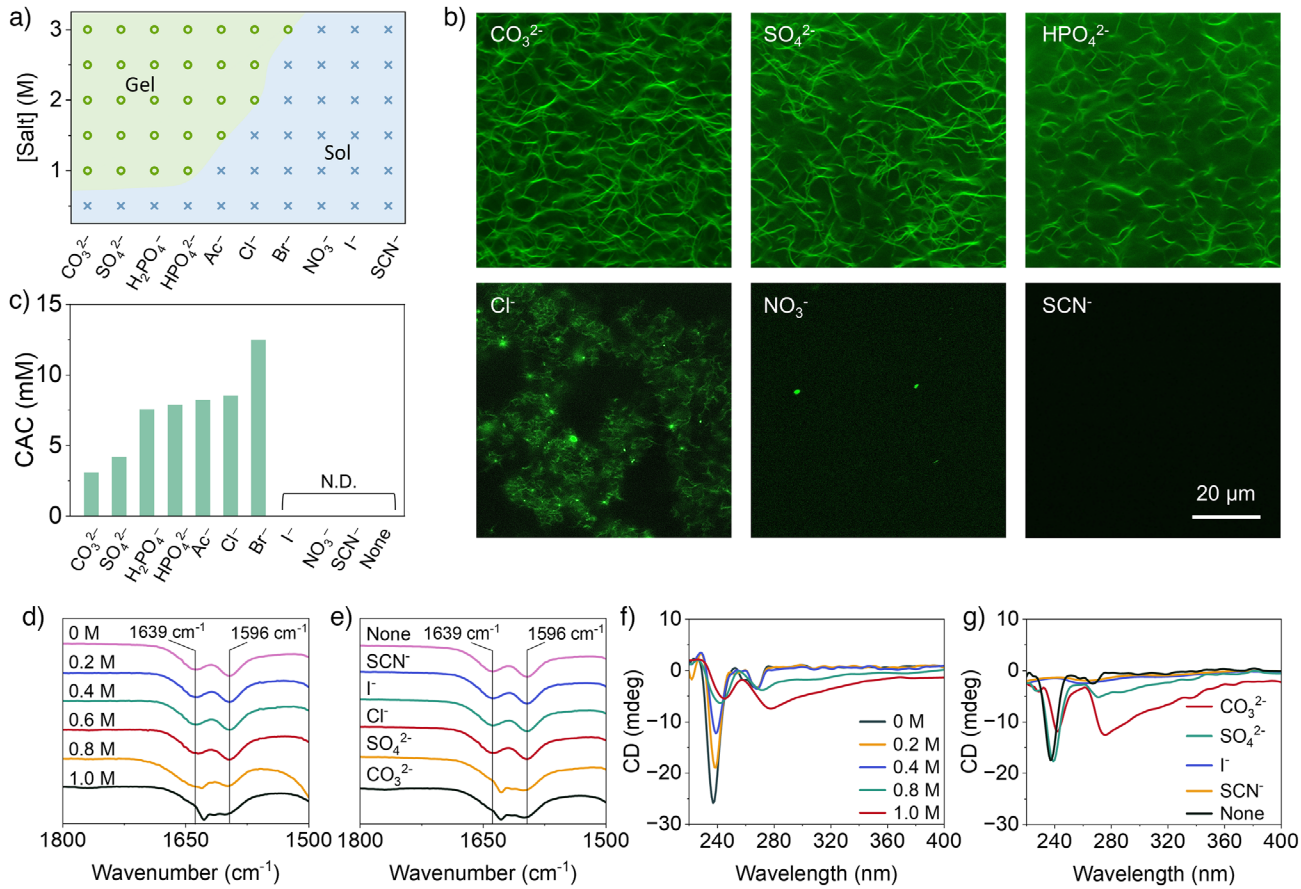

Figure 2. Self-assembly of gelator **3b** driven by kosmotropic anions. a) Hydrogelation diagram in the presence of different anions. b) Confocal microscopy images showing the self-assembled structures of gelator **3b**, [**3b**] = 30 mM. c) CAC of **3b** in the presence of different anions, N.D. means not detected. FTIR spectra of gelator **3b** in the presence of d) varying [CO_3^{2-}] and e) different anions. CD spectra of gelator **3b** in the presence of f) varying [CO_3^{2-}] and g) different anions, [**3b**] = 5 mM. Unless stated otherwise, [salt] = 1.0 M and [**3b**] = 60 mM at pH 8.0.

chaotropic anions, NO_3^-, I^-, and SCN^-, also suggesting that the self-assembly of **3b** in the presence of kosmotropic anions is not caused by electrostatic effect. Confocal microscopy observations demonstrate that the formed hydrogels of **3b** show similar fibrous networks to that of **3a** formed at pH 3.0 (Figures 2b and S8), and ions closer to the left of the Hofmeister series give rise to denser networks.

To detail the effect of these anions on the self-assembly of **3b**, critical aggregation concentration (CAC) of **3b** in the presence of different anions was measured (see Supporting Information), which is found to follow the Hofmeister series as well, increasing from 3 mM for CO_3^{2-} to 13 mM for Br^- (Figures 2c and S9). As a comparison, no aggregations were detected in the samples containing chaotropic anions, NO_3^-, I^-, and SCN^-. We also examined the effect of cations (chloride salts) on the self-assembly of **3b**. The results show that, except for NH_4^+, the cation with smaller diameter contribute more to the self-assembly (Figure S10), suggesting that the effect of cations on the self-assembly is mainly derived from electrostatic effect. In considering of the rather weak Hofmeister effect of cations relative to the anions,[68,69] unless mentioned otherwise, we just focus on anions (sodium salts) in the following study.

To further insight into the self-assembly mechanism of gelator **3b** triggered by kosmotropic anions, Fourier transform infrared spectroscopy (FTIR) was performed to monitor the variation of intermolecular interactions (see Supporting Information). The absorbance at 1596 cm^{-1} is assigned to the deprotonated carboxylates. With the increase in [CO_3^{2-}], the characteristic absorbance of amide I band shifts from 1639 to 1629 cm^{-1} (Figure 2d), indicating the formation of intermolecular hydrogen bonds, which is responsible for the self-assembly of **3b**. Conversely, negligible influence on the absorbance of amide I band was observed for chaotropic anions (Figure 2e). Circular dichroism (CD) measurements also evidence such effects of ions on the self-assembly of **3b**.[70] With increase in [CO_3^{2-}], a broad negative Cotton effect in the range of 260–360 nm is observed (Figure 2f), which is caused by the generation of π–π stacking interactions.[71] Furthermore, the Cotton effect at 237 nm shows a redshift, indicating the occurrence of self-assembly, which is similar to the self-assembly of **3a** (Figure S11).[72] In contrast, the samples with addition of chaotropic ions show CD silence (Figures 2g and S12), suggesting the absence of self-assembly. These results demonstrate that sufficient noncovalent interactions between the molecules of gelator

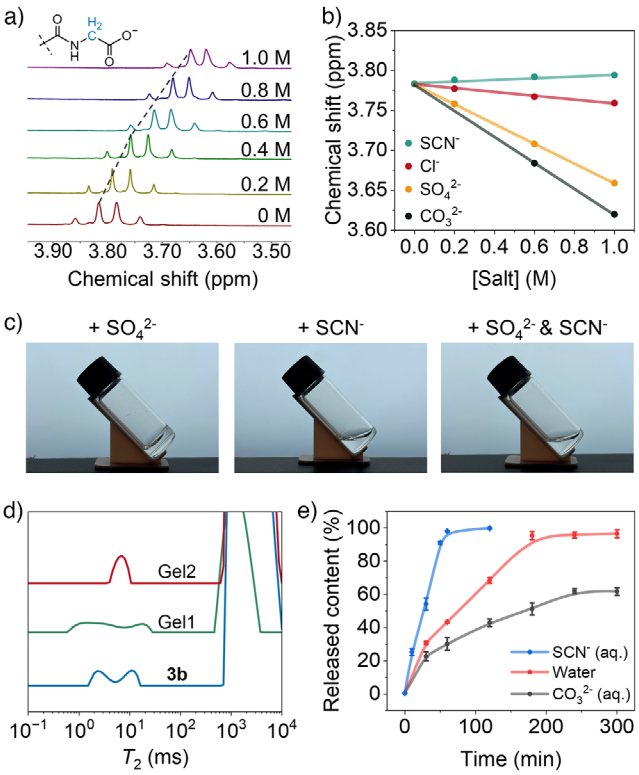

Figure 3. Mechanic study of the Hofmeister effect–mediated self-assembly of **3b**. a) ^{1}H NMR spectra of glycine methylene in **3b** at different [CO_3^{2-}], pD = 8.0. b) ^{1}H NMR chemical shifts of the glycine methylene in **3b** against the concentration of different anions. c) Photographs showing the hydrogelation behavior of **3b** in the presence of SO_4^{2-}, SCN^-, and SO_4^{2-} + SCN^-, respectively. (d) Low-field ^{1}H NMR spectra of gelator **3b**, Gel1, and Gel2. e) Disintegration of Gel2 triggered by diffusion of CO_3^{2-} and the addition of SCN^- for controlled release of model drug bromocresol purple (2.0 mM), error bars represent SD from three independent experiments. Samples: [**3b**] = 15 mM in (a) and b) and 60 mM in (c)–(e); unless stated otherwise, [salt] = 1.0 M.

3b are well formed in the presence of kosmotropic anions, thereby driving the self-assembly of gelator **3b** into the observed hydrogel fibers.

It has been proposed that the Hofmeister effect is caused by the ion-reorganized hydration in bulk or direct interaction between the ions and solutes. To obtain further insight into the facilitated self-assembly of **3b** by kosmotropic anions, ^{1}H NMR tests on gelator **3b** with different [CO_3^{2-}] and different anions were performed. As shown in Figure 3a, increase in [CO_3^{2-}] renders the chemical shift of the glycine methylene protons in **3b** to lower values. It appears that the highly hydrated CO_3^{2-} polarizes surrounding H_2O, thereby disrupting the hydrogen bonding between H_2O and gelator **3b**, thus decreasing the solvation effect and allowing for formation of sufficient intermolecular interactions which drive the self-assembly of **3b** (Figure 1b).[7,73–75] Indeed, the glycine moieties are fully hydrated, and the carbonyl oxygen serve as hydrogen bond acceptor for the surrounding H_2O. Upon the disruption of the interaction between carbonyl oxygen and H_2O by CO_3^{2-}, the electron-withdrawing effect of H_2O on the carbonyl oxygen vanishes, leading to increase in electron density at the oxygen atom, which leads the chemical shift of the adjacent methylene protons to lower values.[76] Moreover, the decrease in chemical shift with the increase in [CO_3^{2-}] follows a linear relationship, indicating that CO_3^{2-} reorganize the water structure without interacting with glycine methylene.[77] Similar variation of chemical shift is observed in other kosmotropic anions and the effect follows the Hofmeister series (Figure 3b). It should be noted that comparable upfield change in chemical shift remains to be observed even at a gelator concentration below the CAC, and the aggregation of gelator **3b** shows slight contribution to the change (Figure S13). In the case of chaotropic anion SCN^-, the chemical shift shows a slight linear increase, indicating the accelerated hydration effect on the gelator. Furthermore, to the hydrogel of **3b** formed with 1.0 M CO_3^{2-}, the addition of equal amount of SCN^- can effectively neutralize the Hofmeister effect, therefore leading to liquification of the hydrogel (Figure 3c), further indicating their antagonistic hydration effect on the gelator.

To further probe the effect of the anions on hydration structure, we conducted low-field ^{1}H NMR measurements to investigate the water species by measuring the spin–spin relaxation time of protons.[78–81] Typically, longer transverse relaxation time (T_2) signifies higher motility of water. As shown in Figure 3d, two distinct bound water peaks (T_2 = 2 and 11 ms, respectively) were observed, which can be attributed to the interactions of carbonyl oxygen–water and carbonate–water, respectively. For Gel2 of **3b** formed with CO_3^{2-}, the peak of bound water at T_2 = 2 ms disappears. This seems to be caused by the competition of kosmotropic CO_3^{2-} with the carbonyl groups for hydration. The shift of T_2 from 11 to 7 ms indicates a decreased mobility of the water, which can be explained by the self-assembly of **3b**, thus limiting the motility of water. As a control, in the case of Gel1 formed by the self-assembly of **3a** without the presence of any kosmotropic anions, the two peaks remain visible except for a largely shifting and broadening, which is caused by the formation of fibrous network. This low-field ^{1}H NMR results further indicate that the presence of kosmotropic anions reorganizes the hydration structure, thus facilitating the self-assembly of **3b**.

By virtue of above findings, we speculated that Gel2 will disintegrate if the kosmotropic anions were removed, which would be very useful for many applications such as drug delivery. To test this hypothesis, Gel2 was soaked in pure water to remove CO_3^{2-} through diffusion. We found that Gel2 gradually disintegrated over time and completely dissolved after 3 h (Figure S14). By loading bromocresol purple into Gel2 as a model drug (see Supporting Information), the hydrogel can rapidly release drug and finish 100% release at 3 h through time-dependent disintegration (Figures 3e and S14). Moreover, upon an incubation with the chaotropic anion SCN^-, the drug can be released even faster, reaching a 100% release at 1 h. Such a faster release rate can be explained by the neutralized Hofmeister effect as discussed above. In contrast, by soaking CO_3^{2-} solution at an equal concentration to Gel2, the hydrogel remains intact over 3 h, and the release of bromocresol purple is rather limited. These results suggest that such Hofmeister effect–mediated supramolecular

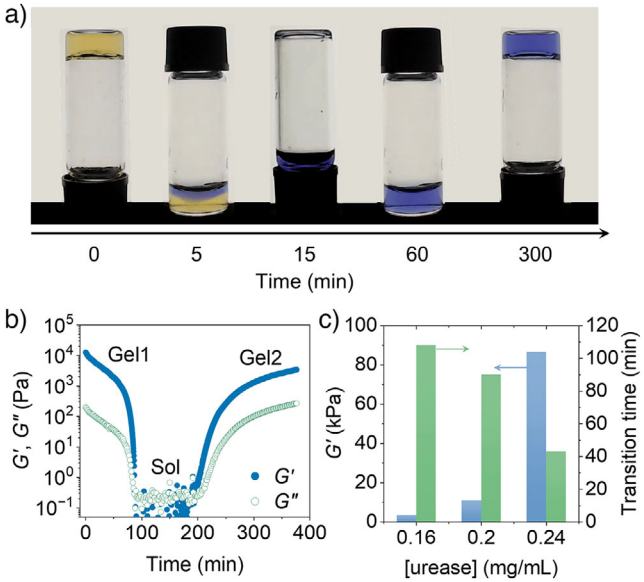

Figure 4. Hofmeister effect–mediated dynamic gel–sol–gel transition. a) Time-dependent gel–sol–gel transition process triggered by urease with 50 μM bromocresol purple as a pH indicator. b) Time-sweep rheological test showing the dynamic gel–sol–gel transition process. c) Stiffness of Gel2 and transition time at different [urease]. Samples: initial pH 5.0, [**3a**] = 60 mM, [urea] = 1.0 M, [urease] = 0.16 mg mL^{-1}.

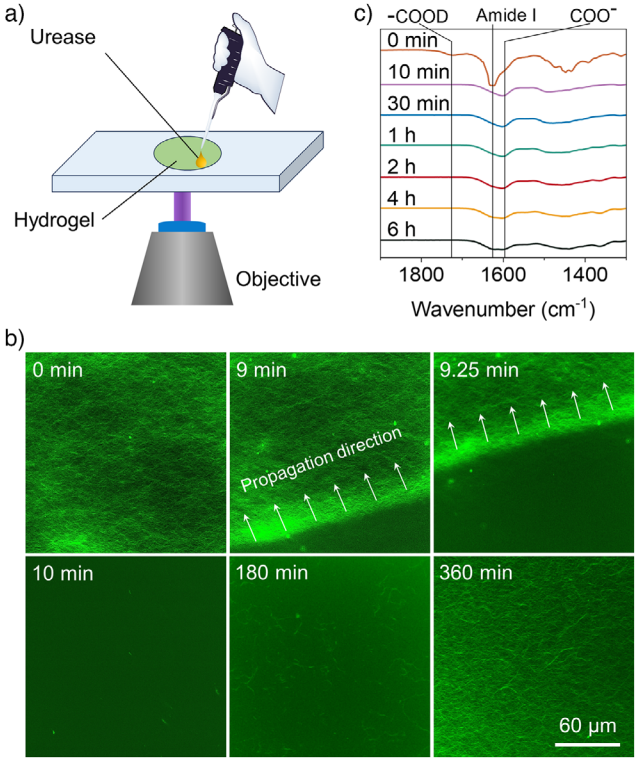

Figure 5. Mechanic insight into the dynamic gel–sol–gel transition process. a) Experimental setup for the in situ confocal microscopy observations. b) Confocal images showing the dynamic evolution process of the hydrogel networks. c) Time-dependent FTIR spectra probing the dynamic evolution of molecular structures and intermolecular interactions of gelator **3**. Samples: initial pH 5.0, [**3a**] = 60 mM, [urea] = 1.0 M, [urease] = 0.16 mg mL^{-1}.

hydrogels may serve as a drug reservoir in the body and release the loaded drugs through the diffusion of kosmotropic anions.

The results we discussed so far demonstrate that kosmotropic anions can drive the self-assembly of gelator **3b** into Gel2 though **3b** is charged. It has been known that **3a**, protonated state of **3**, can self-assemble into Gel1. Therefore, we hypothesize that a self-regulating transition from Gel1 to Gel2 can be expected if we can couple the self-assembly of **3** to a chemical reaction system that can simultaneously produce base and kosmotropic anions. It seems that the hydrolysis of urea to release NH_3 and CO_2 under the catalysis of urease can fulfill these requirements. The produced basic NH_3 can covert Gel1 to a sol because of the deprotonation of **3a**, however, with the accumulation of kosmotropic ions, NH_4^+ and CO_3^{2-}, the deprotonated **3b** will be driven to self-assemble into Gel2 (Figure 1b).

To examine this hypothesis, we prepared Gel1 containing 60 mM gelator **3a** and 1.0 M urea (see Supporting Information). The concentration of urea is selected to ensure the formation of Gel2 after a complete hydrolysis (Figure S15). To trace the pH variation in the hydrogel, 50 μM bromocresol purple was added as a pH indicator. After adding 0.16 mg mL^{-1} urease on the top of Gel1, purple color propagating from the hydrogel surface to the bulk was observed, indicating the formation of basic NH_3, and the hydrogel converted to sol within 15 min because of the deprotonation of **3a** (Figure 4a and Movie S2). However, interestingly, the resultant purple solution is further converted to a self-supporting hydrogel after 300 min, which can be explained by the accumulation of kosmotropic ions, NH_4^+ and CO_3^{2-}. As such, self-regulating gel–sol–gel transition relying on Hofmeister effect is realized.

Oscillatory rheological measurements were further performed to study the dynamic gel–sol–gel transition process (see Supporting Information). We observed that the preformed Gel1 of **3a** with a G' of ~120 kPa started to disintegrate after the addition of urease and was completely liquified at ~85 min (Figure 4b). Interestingly, after a stay at the liquid state for ~108 min, a new hydrogelation process was observed, resulting in a hydrogel with G' of ~3.0 kPa at the time of 360 min. These rheological results are consistent with the above-discussed dynamic gel–sol–gel transition process. Furthermore, the stiffness of the resultant Gel2 as well as the time of the whole transition process can be well controlled, varying from ~3.0 to ~86 kPa and ~108 to ~43 min, respectively, by increasing [urease] from 0.16 to 0.24 mg mL^{-1} (Figures 4c and S16). The increase in stiffness with more urease can be explained by the facilitating self-assembly that leads to more branched growth of supramolecular fibers,[82] while the decrease in transition time is caused by the faster production of base and kosmotropic ions. It should be noted that changing [urea] can also serve as an effective way to regulate the hydrogel stiffness as well as the transition time (Figure S17).

Confocal microscopy observations were further performed to gain more details of the dynamic gel–sol–gel transition process (see Supporting Information and Figure 5a). In

the beginning, fibrous network of Gel1 self-assembled by **3a** was visualized. After the addition of urease at the edge of the confocal cuvette (Figure 5a), the fibrous network disintegrates unidirectionally (Figure 5b and Movie S3), which is caused by the directional diffusion of basic NH_3 produced by the enzymatic hydrolysis of urea. Interestingly, after a period of silence, new coarse fibrous network is formed. The fibrous structures with a comparable diameter of ~10 nm in both Gel1 and Gel2 were confirmed by TEM (Figure S18). This dynamic evolution of fibrous network is in agreement with the aforementioned macroscopic observations and rheological results.

To obtain molecular insight into the dynamic gel–sol–gel transition process, FTIR spectroscopy was employed to monitor the evolution of intermolecular interactions (see Supporting Information and Figure S19). For the sample of Gel1, as shown in Figure 5c, a peak at 1724 cm^{-1} assigned to the protonated carboxylic acid groups (—COOD) of gelator **3a** was observed, and the amide I band at 1627 cm^{-1} indicated the self-assembly of **3a**. Ten min after the addition of urease, the peak at 1724 cm^{-1} disappeared and a new peak was visible at 1600 cm^{-1}, indicating the formation of deprotonated carboxylate groups (—COO^-) due to the production of basic NH_3. Moreover, the amide I band became inconspicuous, manifesting the disassembly of Gel1. However, over time, the absorbance intensity of amide I band at 1627 cm^{-1} gradually increases, indicating the self-assembly of **3b** driven by the formed kosmotropic ions. These FTIR data clearly shows the dynamic evolution process of molecular structures and intermolecular interactions of gelator **3**, dominating the above-observed dynamic gel–sol–gel transition process.

Conclusion

In summary, we have demonstrated how Hofmeister effect can be orchestrated to realize self-regulating gel–sol–gel transition through a simple enzymatic reaction. We find that kosmotropic anions can effectively drive the self-assembly of carbonates-containing gelators into hydrogels; even the gelators are charged through deprotonation at basic pH. Our study suggests that the self-assembly of dissociated gelators is caused by the disruption of gelator–water interactions by kosmotropic anions. Interestingly, by coupling the Hofmeister effect–mediated self-assembly with enzymatic hydrolysis of urea, the hydrogels formed at acidic pH disassemble into sol because of the generation of basic NH_3; however, over time, with the production and accumulation of kosmotropic ions, NH_4^+ and CO_3^{2-}, the dissociated gelators are further accelerated to self-assemble into new hydrogels. As such, to our best knowledge, we demonstrate the first example of self-regulating gel–sol–gel transition using Hofmeister effect. Our findings verify that Hofmeister effect can effectively regulate intermolecular interactions to retain molecular assemblies, which sheds light on the understanding of specific ion effect in nature, for instance, the survival of halophilic organisms in extreme saline conditions.[83–86] More importantly, such Hofmeister effect–mediated dynamic supramolecular self-assembly offers a new opportunity for the creation of lifelike self-regulating soft materials for applications such as ion-programmed biosensing and drug delivery.

Acknowledgements

The authors acknowledge the financial support of the Natural Science Foundation of Shanghai (22ZR1417700), the Science Fund for Creative Research Groups of the Natural Science Foundation of China (52321002 and 21908061), and the Shanghai Pilot Program for Basic Research (22TQ1400100-9). The authors would like to express our gratitude to Prof. Shengtong Sun and Ms. Ying Zhao from Donghua University for their assistance with low-field ^1H NMR measurements.

Conflict of Interests

The authors declare no conflict of interest.

Data Availability Statement

The data that support the findings of this study are available in the Supporting Information of this article.

Keywords: Dynamic gelation · Hofmeister effect · Low-molecular-weight gelators · Self-assembly · Supramolecular chemistry

[1] F. Hofmeister, *Arch. Exp. Pathol. Pharmakol.* **1888**, *24*, 247–260.
[2] W. Kunz, J. Henle, B. W. Ninham, *Curr. Opin. Colloid Inter. Sci.* **2004**, *9*, 19–37.
[3] P. K. Grover, R. L. Ryall, *Chem. Rev.* **2005**, *105*, 1–10.
[4] Y. Marcus, *Chem. Rev.* **2009**, *109*, 1346–1370.
[5] Y. Zhang, P. S. Cremer, *Curr. Opin. Chem. Biol.* **2006**, *10*, 658–663.
[6] P. Jungwirth, P. S. Cremer, *Nat. Chem.* **2014**, *6*, 261–263.
[7] K. D. Collins, M. W. Washabaugh, *Q. Rev. Biophys.* **1985**, *18*, 323–422.
[8] A. W. Omta, M. F. Kropman, S. Woutersen, H. J. Bakker, *Science* **2003**, *301*, 347–349.
[9] J. D. Smith, R. J. Saykally, P. L. Geissler, *J. Am. Chem. Soc.* **2007**, *129*, 13847–13856.
[10] Y. Zhang, S. Furyk, D. E. Bergbreiter, P. S. Cremer, *J. Am. Chem. Soc.* **2005**, *127*, 14505–14510.
[11] V. J. Nebot, J. J. Ojeda-Flores, J. Smets, S. Fernández-Prieto, B. Escuder, J. F. Miravet, *Chem. Eur. J.* **2014**, *20*, 14465–14472.
[12] C. G. Pappas, R. Shafi, I. R. Sasselli, H. Siccardi, T. Wang, V. Narang, R. Abzalimov, N. Wijerathne, R. V. Ulijn, *Nat. Nanotechnol.* **2016**, *11*, 960–967.
[13] Y. Li, Y. Wang, G. Huang, X. Ma, K. Zhou, J. Gao, *Angew. Chem. Int. Ed.* **2014**, *53*, 8074–8078.
[14] Y. Du, J. Shen, H. Li, Y. Jiang, X. Liu, W. Hua, N. Yan, *J. Colloid Inter. Sci.* **2025**, *686*, 672–680.
[15] N. Mittal, T. Benselfelt, F. Ansari, K. Gordeyeva, S. V. Roth, L. Wågberg, L. Soderberg, *Angew. Chem. Int. Ed.* **2019**, *58*, 18562–18569.
[16] K. Li, J. Yang, J. Gu, *Chem. Sci.* **2019**, *10*, 5743–5748.
[17] S. Paul, K. Gayen, P. G. Cantavella, B. Escuder, N. Singh, *Angew. Chem. Int. Ed.* **2024**, *63*, e202406220.

[18] S. A. P. van Rossum, M. Tena-Solsona, J. H. van Esch, R. Eelkema, J. Boekhoven, *Chem. Soc. Rev.* **2017**, *46*, 5519–5535.
[19] R. Merindol, A. Walther, *Chem. Soc. Rev.* **2017**, *46*, 5588–5619.
[20] G. Ragazzon, L. J. Prins, *Nat. Nanotechnol.* **2018**, *13*, 882–889.
[21] Q. Wang, Z. Qi, M. Chen, D.-H. Qu, *Aggregate* **2021**, *2*, e110.
[22] S. De, R. Klajn, *Adv. Mater.* **2018**, *30*, 1706750.
[23] E. te Brinke, J. Groen, A. Herrmann, H. A. Heus, G. Rivas, E. Spruijt, W. T. S. Huck, *Nat. Nanotechnol.* **2018**, *13*, 849–855.
[24] W. R. Berg, J. F. Berengut, C. Bai, L. Wimberger, L. K. Lee, F. J. Rizzuto, *Angew. Chem. Int. Ed.* **2023**, *62*, e202314458.
[25] O. Zozulia, C. M. E. Kriebisch, B. A. K. Kriebisch, H. Soria-Carrera, K. R. Ryadi, J. Steck, J. Boekhoven, *Angew. Chem. Int. Ed.* **2024**, *63*, e202407424.
[26] P. Zambrano, X. Chen, C. M. E. Kriebisch, B. A. K. Kriebisch, O. Zozulia, J. Boekhoven, *J. Am. Chem. Soc.* **2024**, *146*, 33359–33367.
[27] R. S. M. Rikken, H. Engelkamp, R. J. M. Nolte, J. C. Maan, J. C. M. van Hest, D. A. Wilson, P. C. M. Christianen, *Nat. Commun.* **2016**, *7*, 12606.
[28] S. Maiti, I. Fortunati, C. Ferrante, P. Scrimin, L. J. Prins, *Nat. Chem.* **2016**, *8*, 725–731.
[29] T. M. Hermans, N. Singh, *Angew. Chem. Int. Ed.* **2023**, *62*, e202301529.
[30] A. Sarkar, B. Dúzs, A. Walther, *J. Am. Chem. Soc.* **2024**, *146*, 10281–10285.
[31] J. Boekhoven, W. E. Hendriksen, G. J. M. Koper, R. Eelkema, J. H. van Esch, *Science* **2015**, *349*, 1075–1079.
[32] H. Xu, S. Bai, G. Gu, Y. Gao, X. Sun, X. Guo, F. Xuan, Y. Wang, *ACS Appl. Mater. Inter.* **2022**, *14*, 43825–43832.
[33] H. Kar, L. Goldin, D. Frezzato, L. J. Prins, *Angew. Chem. Int. Ed.* **2024**, *63*, e202404583.
[34] S. M. Poprawa, M. Stasi, B. A. K. Kriebisch, M. Wenisch, J. Sastre, J. Boekhoven, *Nat. Commun.* **2024**, *15*, 4204.
[35] A.-L. Holtmannspötter, C. Machatzke, C. Begemann, E. Salibi, C. Donau, F. Späth, J. Boekhoven, H. Mutschler, *Angew. Chem. Int. Ed.* **2024**, *63*, e202412534.
[36] F. Späth, A. S. Maier, M. Stasi, A. M. Bergmann, K. Halama, M. Wenisch, B. Rieger, J. Boekhoven, *Angew. Chem. Int. Ed.* **2023**, *62*, e202309318.
[37] J. Boekhoven, A. M. Brizard, K. N. K. Kowlgi, G. J. M. Koper, R. Eelkema, J. H. van Esch, *Angew. Chem. Int. Ed.* **2010**, *49*, 4825–4828.
[38] B. G. P. van Ravensteijn, W. E. Hendriksen, R. Eelkema, J. H. van Esch, W. K. Kegel, *J. Am. Chem. Soc.* **2017**, *139*, 9763–9766.
[39] S. Bal, C. Ghosh, T. Ghosh, R. K. Vijayaraghavan, D. Das, *Angew. Chem. Int. Ed.* **2020**, *59*, 13506–13510.
[40] M. M. Hossain, J. L. Atkinson, C. S. Hartley, *Angew. Chem. Int. Ed.* **2020**, *59*, 13807–13813.
[41] Z. Zong, Q. Zhang, S.-H. Qiu, Q. Wang, C. Zhao, C.-X. Zhao, H. Tian, D.-H. Qu, *Angew. Chem. Int. Ed.* **2022**, *61*, e202116414.
[42] X. Chen, M. Stasi, J. Rodon-Fores, P. F. Großmann, A. M. Bergmann, K. Dai, M. Tena-Solsona, B. Rieger, J. Boekhoven, *J. Am. Chem. Soc.* **2023**, *145*, 6880–6887.
[43] S. Maiti, I. Fortunati, C. Ferrante, P. Scrimin, L. J. Prins, *Nat. Chem.* **2016**, *8*, 725–731.
[44] T. Bian, A. Gardin, J. Gemen, L. Houben, C. Perego, B. Lee, N. Elad, Z. Chu, G. M. Pavan, R. Klajn, *Nat. Chem.* **2021**, *13*, 940–949.
[45] T. Marchetti, B. M. W. Roberts, D. Frezzato, L. J. Prins, *Angew. Chem. Int. Ed.* **2024**, *63*, e202402965.
[46] C. Pan, J. Xu, L. Wang, Y. Jia, J. Li, G. Liu, S. Zhu, B. Yang, Y. Li, *CCS Chem* **2023**, *5*, 669–681.
[47] H. Kar, R. Chen, K. Das, L. J. Prins, *Angew. Chem. Int. Ed.* **2025**, *64*, e202414495.
[48] T. Heuser, E. Weyandt, A. Walther, *Angew. Chem. Int. Ed.* **2015**, *54*, 13258–13262.
[49] S. Panja, B. Dietrich, O. Shebanova, A. J. Smith, D. J. Adams, *Angew. Chem. Int. Ed.* **2021**, *60*, 9973–9977.
[50] P. Ravarino, S. Panja, S. Bianco, T. Koev, M. Wallace, D. J. Adams, *Angew. Chem. Int. Ed.* **2023**, *62*, e202215813.
[51] Z. Wang, T. Zhao, S. Yang, Y. Meng, X. Wang, *CCS Chem* **2024**, *6*, 1951–1964.
[52] G. Ragazzon, M. Baroncini, S. Silvi, M. Venturi, A. Credi, *Nat. Nanotechnol.* **2015**, *10*, 70–75.
[53] M. Kathan, F. Eisenreich, C. Jurissek, A. Dallmann, J. Gurke, S. Hecht, *Nat. Chem.* **2018**, *10*, 1031–1036.
[54] X. Yang, W. Shi, Z. Chen, M. Du, S. Xiao, S. Qu, C. Li, *Adv. Funct. Mater.* **2023**, *33*, 2214394.
[55] C. Li, A. Iscen, H. Sai, K. Sato, N. A. Sather, S. M. Chin, Z. Álvarez, L. C. Palmer, G. C. Schatz, S. I. Stupp, *Nat. Mater.* **2020**, *19*, 900–909.
[56] D. Barpuzary, P. J. Hurst, J. P. Patterson, Z. Guan, *J. Am. Chem. Soc.* **2023**, *145*, 3727–3735.
[57] S. Selmani, E. Schwartz, J. T. Mulvey, H. Wei, A. Grosvirt-Dramen, W. Gibson, A. I. Hochbaum, J. P. Patterson, R. Ragan, Z. Guan, *J. Am. Chem. Soc.* **2022**, *144*, 7844–7851.
[58] Q. Yan, Y. Zhao, *J. Am. Chem. Soc.* **2013**, *135*, 16300–16303.
[59] Q. Yan, R. Zhou, C. Fu, H. Zhang, Y. Yin, J. Yuan, *Angew. Chem. Int. Ed.* **2011**, *50*, 4923–4927.
[60] Y. Wang, Q. Yan, *Angew. Chem. Int. Ed.* **2023**, *62*, e202217001.
[61] H. Wang, X. Fu, G. Gu, S. Bai, R. Li, W. Zhong, X. Guo, R. Eelkema, J. H. van Esch, Z. Cao, Y. Wang, *Angew. Chem. Int. Ed.* **2023**, *62*, e202310162.
[62] S. Bai, H. Wang, G. Gu, J. Zhang, L. Wei, Y. Gao, Z. Li, X. Guo, Y. Wang, *ACS Mater. Lett.* **2023**, *5*, 2377–2383.
[63] H. Wang, K. Wang, S. Bai, L. Wei, Y. Gao, K. Zhi, X. Guo, Y. Wang, *J. Colloid Inter. Sci.* **2024**, *664*, 938–945.
[64] X. Fan, A. Walther, *Angew. Chem. Int. Ed.* **2021**, *60*, 3619–3624.
[65] Y. Zhao, B. Li, X. Fu, P. Zhao, Y. Zhao, W. Zhou, Y. Lu, Y. Zheng, *Angew. Chem. Int. Ed.* **2025**, *64*, e202415582.
[66] K. A. Dill, *Biochemistry* **1990**, *29*, 7133–7155.
[67] P. L. Nostro, B. W. Ninham, *Chem. Rev.* **2012**, *112*, 2286–2322.
[68] K. P. Gregory, G. R. Elliott, H. Robertson, A. Kumar, E. J. Wanless, G. B. Webber, V. S. J. Craig, G. G. Andersson, A. J. Page, *Phys. Chem. Chem. Phys.* **2022**, *24*, 12682–12718.
[69] H. I. Okur, J. Kherb, P. S. Cremer, *J. Am. Chem. Soc.* **2013**, *135*, 5062–5067.
[70] M. Liu, L. Zhang, T. Wang, *Chem. Rev.* **2015**, *115*, 7304–7397.
[71] H. Jiang, Y. Jiang, J. Han, L. Zhang, M. Liu, *Angew. Chem. Int. Ed.* **2019**, *58*, 785–790.
[72] L. Yang, F. Wang, D. Y. Auphedeous, C. Feng, *Nanoscale* **2019**, *11*, 14210–14215.
[73] B. Hribar, N. T. Southall, V. Vlachy, K. A. Dill, *J. Am. Chem. Soc.* **2002**, *124*, 12302–12311.
[74] A. S. Thomas, A. H. Elcock, *J. Am. Chem. Soc.* **2007**, *129*, 14887–14898.
[75] A. Acharyya, D. Mukherjee, F. Gai, *J. Phys. Chem. B* **2020**, *124*, 11783–11792.
[76] B. A. Rogers, H. I. Okur, C. Yan, T. Yang, J. Heyda, P. S. Cremer, *Nat. Chem.* **2022**, *14*, 40–45.
[77] H. Wang, H. Su, T. Xu, H. Cui, *Angew. Chem. Int. Ed.* **2023**, *62*, e202306652.
[78] W.-H. Zhang, M.-J. Yin, Q. Zhao, C.-G. Jin, N. Wang, S. Ji, C. L. Ritt, M. Elimelech, Q.-F. An, *Nat. Nanotechnol.* **2021**, *16*, 337–343.
[79] J. Wei, G. Wei, Y. Shang, J. Zhou, C. Wu, Q. Wang, *Adv. Mater.* **2019**, *31*, 1900248.
[80] H. Huang, L. Han, X. Fu, Y. Wang, Z. Yang, L. Pan, M. Xu, *Small* **2021**, *17*, 2006807.
[81] K. Gong, L. Hou, P. Wu, *Adv. Mater.* **2022**, *34*, 2201065.

[82] J. Boekhoven, J. M. Poolman, C. Maity, F. Li, L. van der Mee, C. B. Minkenberg, E. Mendes, J. H. van Esch, R. Eelkema, *Nat. Chem.* **2013**, *5*, 433–437.
[83] X. Tadeo, B. López-Méndez, T. Trigueros, A. Laín, D. Castaño, O. Millet, *PLoS Biol.* **2009**, *7*, e1000257.
[84] R. Margesin, F. Schinner, *Extremophiles* **2001**, *5*, 73–83.
[85] R. Munns, M. Tester, *Annu. Rev. Plant Biol.* **2024**, *51*, 16–34.
[86] H. Zhou, H. Shi, Y. Yang, X. Feng, X. Chen, F. Xiao, H. Lin, Y. Guo, *J. Genet. Genomics* **2024**, *51*, 16–34.

Manuscript received: March 07, 2025
Revised manuscript received: April 11, 2025
Accepted manuscript online: April 22, 2025
Version of record online: April 27, 2025